Indian Journal of Chemical Technology
Vol. 19, May 2012, pp. 195-204

Theoretical and electrochemical studies on the effect of substitution on 1, 2, 4- triazole towards mild steel corrosion inhibition in hydrochloric acid

Sam John & Abraham Joseph*
Department of Chemistry, University of Calicut, Calicut 673 635, India

Received 27 May 2011; accepted 21 February 2012

The present paper reports study on the inhibition of mild steel in 0.5 M HCl with different concentrations of substituted 1,2,4-triazoles using conventional weight loss method, potentiodynamic polarization studies, linear polarization studies, electrochemical impedance spectroscopy and quantum chemical calculations. The theoretical study has been initiated using density functional theory at the B3LYP/6-31G (d) level in order to elucidate the inhibition efficiencies and reactive sites of these inhibitor molecules. The efficiencies of corrosion inhibitors and the global chemical reactivity relate to some parameters, such as E_{HOMO}, E_{LUMO}, gap energy (ΔE), electronegativity (χ), global hardness (η) and the fraction of electrons transferred from inhibitor molecule to the metal atom (ΔN). The calculated results are in good agreement with the experimental data on the whole. In addition, the local reactivity has been analyzed through the Fukui function and condensed softness indices. Results show that the corrosion rate decreases and inhibition efficiency increases with inhibitor concentration. The results of polarization studies reveal that the additive acts as a mixed type inhibitor. The surface adsorption of inhibitor molecules decreases the double layer capacitance and increases the polarization resistance.

Keywords: Corrosion inhibitors, Density functional theory, Electrochemical parameters, Fukui function, Softness indices

Metal corrosion is a fundamental process of vital importance in economics and society. Corrosion inhibition of mild steel is a matter of theoretical and practical importance[1-3]. Mineral acids, particularly hydrochloric acid, frequently used in industrial processes involve acid cleaning, acid pickling, acid descaling and oil well acidizing. Due to aggressiveness of acids, inhibitors are often used to reduce the dissolution of metals[4-7]. Most acid corrosion inhibitors are organic compounds containing hetero atoms or systems with the unsaturated bonds (such as double bonds or triple bonds) or plane conjugated systems including all kinds of aromatic cycles. Schiff base compounds due to the presence of azomethine group show more inhibition efficiency than corresponding amines and carbonyl compounds. More emphasis is being given recently in the investigation of Schiff bases as corrosion inhibitors in acidic media due to their enhanced inhibiting action and easiness of synthesis from relatively cheap raw materials. The adsorption of the inhibitor molecule at the metal solution interface is the first step in the mechanism of inhibitory action. Organic molecules may adsorb on the metal surface by (i) electrostatic interaction between a negatively charged surfaces, which is provided with specifically adsorbed anions (Cl^-) on metal and positive charge of the inhibitor, (ii) interaction of unshared electron pair in the inhibitor molecule with metal, (iii) interaction of pi electron of the inhibitor molecule with the metal and/or, (iv) a combination of all the above processes.

Quantum-chemical calculations found to be quite useful to investigate the electronic properties and reaction mechanisms of the inhibitor molecules[8-13]. The geometry of the inhibitor molecule in its ground state, the nature of its molecular orbital like highest occupied molecular orbital (HOMO) and lowest unoccupied molecular orbital (LUMO) are involved in the inhibition activity. Through density functional theory (DFT) calculations it is possible to correlate inhibition property with ionization potential (I), electron affinity (A), and number of electrons transferred (ΔN). Recently, molecular dynamics simulation studies unveil the mechanism of corrosion inhibition through interaction of molecules with surface metal atoms. The objective of the present study is to find the relationship between structural parameters, such as electronic properties of inhibitors, the frontier molecular orbital energy (E_{HOMO}, E_{LUMO}),

*Corresponding author.
E-mail: drabrahamj@gmail.com

and the charge distribution of the inhibitors and to observe the correlation between the molecular structure and the experimental electro analytical data.

Experimental Procedure

Materials

The mild steel samples of the compositions C= 0.2%, Mn= 1%, P= 0.03%, S= 0.02%, and Fe= 98.75% were used for the study. The mild steel specimens used in weight loss measurements are cut in 4.8×1.9 cm^2 coupons. For electrochemical studies, same types of coupons were used but only 1cm^2 area is exposed during each measurements. Before both the measurements the samples were polished using different grade of emery papers followed by washing with ethanol, acetone and finally distilled water.

Inhibitor

4-Amino-4H-1, 2, 4 triazole-3, 5 dimethanol was prepared by refluxing hydrazine hydrate and glycolic acid (ATD)[14-16]. 4-Amino-3, 5-bis (chloromethyl)-4H-1,2,4 triazole (ACT) was prepared from ATD by reacting the latter with thionyl chloride. The purified and recrystallised sample is characterized by physico-chemical methods. ATD has M.P. 206–208°C; elemental analysis calcd (%) for $C_4H_8N_4O_2$ (144.13): C 33.33, H 5.59, N 38.87; found (%): C 33.29, H 5.41, N 39.05; 1H NMR (300 MHz, [D6]DMSO): d=4.54 (d,3J=6.0 Hz, 4H; 2STzCH_2OH), 5.37 (t,3J=6.0 Hz, 2H; 2STzCH_2OH), 5.81 ppm (s, 2H; TzNH_2), IR (KBr): ν =3344, 3220, 2877, 2687, 1639, 1518, 1479, 1461, 1440, 1379, 1351, 1305,1280, 1204, 1068, 1029, 976, 953, 875, 819, 774, 720, 498 cm^{-1}. ACT has M.P. 139–1418C; elemental analysis calcd (%) for $C_4H_7Cl_3N_4$ (217.48): C 22.09, H 3.24, N 25.76; found (%) : C 22.24, H 3.24, N 25.83;1H NMR (300 MHz, [D6]DMSO): d=4.92 ppm (s, 4H; 2STzCH_2Cl); IR (KBr): ν =3414, 3253, 3145, 2970, 2642, 1637, 1617, 1576, 1417, 1328, 1264, 1165, 1105, 1034, 975, 937, 919, 888, 807, 759, 668, 646, 605, 568, 513 cm^{-1}. These compounds are readily soluble in 0.5M HCl. The structure of the molecule is given in Fig. 1.

Medium

The medium for the study was prepared from reagent grade HCl (E merck) using doubly distilled water. The entire tests were performed in aerated medium in a 250 mL beaker containing acid solution under standard conditions.

Weight loss measurements

The weight loss experiments were carried out under total immersion conditions in test solution maintained at 300 K. For weight loss studies the required number of specimens of 19×48×1 mm size were cut and cleaned in acid solutions and later polished with 1-4/0 finer grades of emery paper to mirror bright finish. All specimens were cleaned according to ASTM standard G-1-72 procedure[17-23]. The experiments were carried out in 250 mL beaker containing the solution. After the exposure period the specimens were removed, washed initially under running tap water, to remove the loosely adhering corrosion product and finally cleaned with mixture of 20%NaOH and 200 g/L zinc dust followed by acetone. Then the loss in weight was determined by analytical balance. The inhibition efficiency (IE%) was obtained using the following equation:

$$\text{IE } \% = \frac{W_0 - W}{W_0} \times 100 \quad \ldots (1)$$

where W_0 and W are the weight losses in the uninhibited and inhibited solution respectively.

Electrochemical measurements

Electrochemical tests were carried out in a conventional three electrode configuration with platinum sheet (1cm^2 surface area) as auxiliary electrode and calomel electrode as the reference electrode. The working electrode was first immersed in the test solution and after establishing a steady state OCP, the electrochemical measurements were carried out in a Gill A C computer controlled

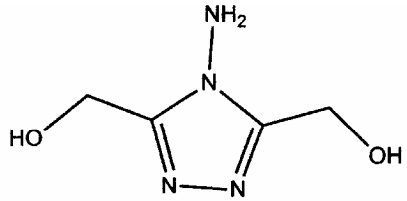

(4-amino-4*H*-1,2,4-triazole-3,5-diyl)dimethanol (ATD)

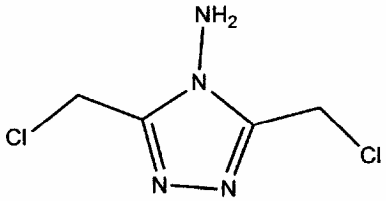

3,5-bis(chloromethyl)-4*H*-1,2,4-triazol-4-amine (ACT)

Fig. 1—Structure of molecules

electrochemical workstation (ACM, UK, model no 1475). Electrochemical impedance spectroscopy (EIS) measurements were carried out with amplitude of 10 mV AC sine wave with the frequency range from 10 KHz to 10Hz. The potentiodynamic polarization curves were obtained in the potential range from–250 mV to +250 mV with a sweep rate of 1 mV/ seconds.

Computational calculations

Among different quantum chemical methods for evaluation of corrosion inhibitors, density functional theory (DFT) has some merits. B3LYP, a version of the DFT method that uses Becke's three-parameter functional (B3) and includes a mixture of HF with DFT exchange terms associated with the gradient corrected correlation functional of Lee, Yang, and Parr (LYP)[24] has been recognized especially for systems containing transition metal atoms[25,26]. It has much less convergence problems than those commonly found for pure DFT methods. Thus, B3LYP was used in the present study to carry out quantum calculations. Then, full geometry optimizations of both the inhibitors were carried out at the B3LYP/6-31G (d) level using the Gaussian 03W program package. Many quantum chemical parameters that indicate structural characteristics of these organic inhibitors, such as E_{HOMO}, E_{LUMO}, energy gap and charge distribution were obtained. DFT also provides a convenient theoretical framework for calculating global and local indices that describe the inherent reactivity of chemical species quantitatively. The electro negativity χ has been identified as the negative of the chemical potential μ, which is the Lagrange multiplier in the differential equation in DFT $\mu = - \chi = (\partial E/\partial N)_{v(r),}$ where E is the total electronic energy, N is the number of electrons[17] and v(r) is the external electrostatic potential that the electrons feel due to the nuclei. The global hardness is defined as $\eta = 1/2(\partial^2 E/\partial N^2)_{v(r)} = (\partial \mu/\partial N)_{v(r)}$ [28] while the global softness S is the inverse of the global hardness[29]. Both χ and η are global properties characterizing the molecules as a whole. The Fukui function $\int(r)$, as proposed by Parr and Yang[30] is defined as the partial derivative of the electron density $\rho(r)$ with respect to the total number of electrons N of the system at the constant external potential v(r): $\int(r), = (\partial E/\partial N)_{v(r).}$ The condensed Fukui function calculations are based on the finite difference approximation and partitioning of the electron density $\rho(r)$ between atoms in a molecular system. Yang and Mortier[31] proposed $\int_k$ calculations from the atomic charges using the following equations:

For reaction with electrophiles

$$\int_k^- = q_N - q_{N-1}, \text{ and} \quad \ldots (2)$$

For reaction with the nucleophiles

$$\int_k^+ = q_{N+1} - q_N \quad \ldots (3)$$

where q_N, q_{N+1} and q_{N-1} are the atomic charges of the systems with N, N+1 and N−1 electrons respectively. The condensed Fukui function is local reactivity descriptor and can be used only for comparing reactive atomic centers within the same molecule. Condensed softness indices allowing the comparison of reactivity between similar atoms of different molecules can be calculated easily starting from the relation between the Fukui function $\int(r)$ and the local softness S (r), as shown below:

$$S(r) = ((\partial \rho(r)/\partial N)_{v(r)} (\partial N/\partial \mu)_{v(r)} = \int(r)S \quad \ldots (4)$$

All calculations, including geometry optimizations of both the structures were performed with the B3LYP exchange correlation corrected functional [32, 33] with the 6-31G (d) basis set using the Gaussian 03W package. As shown by De Proft *et al.*[34], the B3LYP functional appears to be reliable for calculating $\int$ (r) and $\int_k$ indices.

Results and Discussion

Weight loss measurements

Weight loss studies were performed at various time intervals in the absence and presence of different concentrations (10 - 200 ppm) of ATD and ACT. The increase in the inhibitor concentration is accompanied by a decrease in weight loss and corrosion rate and increase in percentage IE. These results lead to the conclusion that both ATD and ACT act as inhibitors for mild steel dissolution in 0.5M HCl solution (Table 1).

Potentiodynamic polarization studies

Anodic and cathodic polarization studies were carried out potentiodynamically in unstirred 0.5M HCl solution in the absence and presence of various concentrations of the inhibitors at 300 K over a potential range from –250mV to +250 mV (Fig. 2). It is clear from the figure that both the anodic metal dissolution and cathodic hydrogen evolution exhibit Tafel type behaviour.

Electrochemical corrosion parameters like corrosion potential (E_{corr}), cathodic and anodic Tafel slopes (β_c and β_a) and corrosion current density (i_{corr}) obtained from Tafel extrapolation of the polarization curve at 300K are given in Table 2. The corrosion inhibition efficiency was calculated using the following relationship:

$$IE\ \% = \frac{I_{Corr^*} - I_{Corr}}{I_{Corr^*}} \times 100 \quad \ldots (5)$$

where I_{corr*} and I_{corr} are the uninhibited and inhibited corrosion current densities respectively. These results suggest that both the compounds (ATD and ACT) act as mixed type inhibitors. The inhibitor molecules are first adsorbed on the mild steel surface, thus blocking the available reaction sites[35-37]. The surface coverage increases with the inhibitor concentration. The LPR trends in the case of ATD and ACT are graphically represented in Fig. 3. The formation of surface inhibitor film on the mild steel surface provides considerable protection to mild steel against corrosion. This film reduces the active surface area exposed to the corrosive medium and delays the hydrogen evolution and iron dissolution.

Table 1—Corrosion rates of mild steel in 0.5N HCl in the presence of ATD and ACT

Inhibitor	Conc., ppm	Corrosion rate, mm/yr			
		24 h	48 h	72 h	96 h
	Blank	1130	507	400	331
	10	624	435	301	277
	50	428	373	278	201
ATD	100	229	178	164	140
	150	123	89	62	50
	200	55	40	39	22
	10	611	419	295	261
	50	396	334	256	221
ACT	100	213	182	151	128
	150	111	78	60	48
	200	53	40	37	25

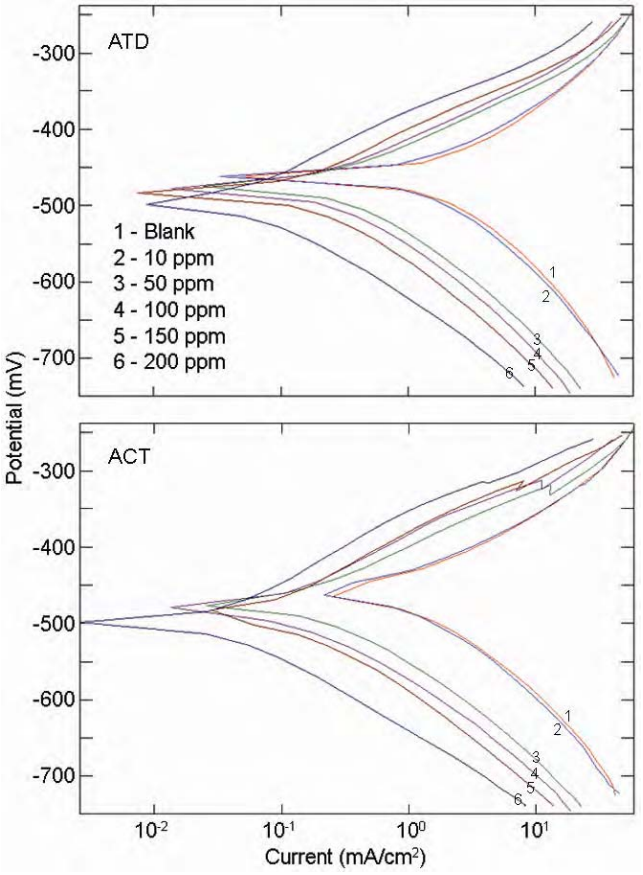

Fig. 2—Polarization curve of MS in 0.5 M HCl in presence of different concentrations of ATD & ACT at 300K

Table 2—Electrochemical parameters for mild steel obtained from polarization curves in 0.5M HCl at 300K (ATD & ACT)

Inhibitor	Conc., ppm	E_{corr} mV	β_a mV dec^{-1}	β_c mV dec^{-1}	i_{corr} μA cm^{-2}	η %	C.R mils/yr
	Blank	481	89	151	0.9651	-	69.74
	10	487	77	144	0.8664	21.44	54.79
ATD	50	484	66	131	0.8113	54.21	31.93
	100	478	60	121	0.7768	64.21	24.95
	150	471	60	98	0.5088	94.22	4.03
	200	456	52	72	0.5000	93.66	4.42
	10	475	69	120	0.7721	81.35	13.00
	50	484	66	73	0.0699	91.51	5.93
ACT	100	478	54	65	0.0478	92.60	5.16
	150	487	40	52	0.0320	89.12	7.53
	200	492	41	41	0.0210	91.36	6.03

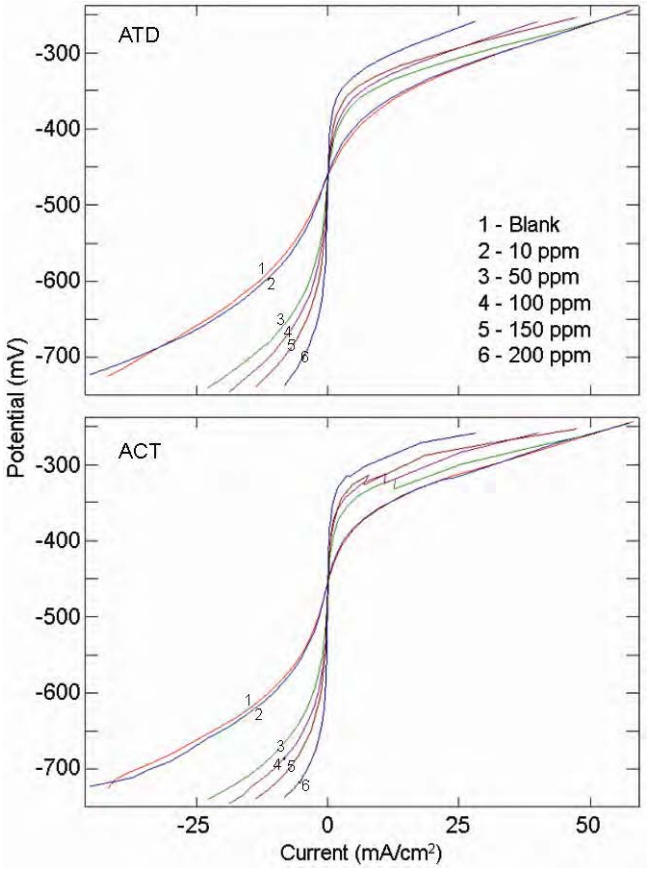

Fig.3—LPR plots for MS in 0.5M HCl in presence of different concentrations of ATD & ACT at 300K

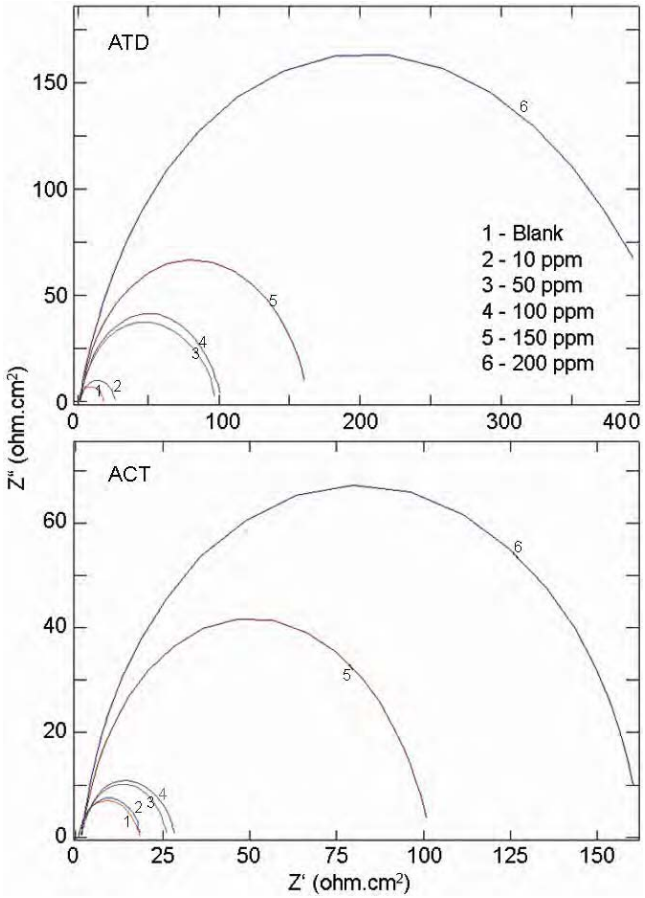

Fig .4—Nyquist plots of MS in 0.5M HCl in presence of different concentrations of ATD & ACT at 300K

Electrochemical impedance spectroscopy

The performance of the organic coatings on the metal surface can be evaluated from the EIS studies. More reliable results can be obtained from this technique as it does not disturb the double layer at the metal/solution interface[38,39]. The Nyquist plots for the MS in uninhibited 0.5 M HCl and those containing various inhibitor concentrations ATD and ACT after 1 h of immersion are given in Fig. 4. It is clear from these figures that in uninhibited solution, Nyquist plot yields a slightly depressed semi circles and the representative Bode (Fig. 5) diagrams give only one time constant. This indicates the corrosion of the MS in the absence of inhibitor, mainly controlled by a charge transfer process. In the evaluation of Nyquist plots, the difference in real impedance at lower and higher frequencies is commonly considered as a charge transfer resistance. The charge transfer resistance must be corresponding to the resistance between the metal and the OHP (Outer Helmholtz Plane). The contribution of all resistances correspond to the metal/solution interface, i.e. charge transfer resistance (R_{ct}), diffuse layer resistance (R_d), accumulation resistance (R_a) and film resistance (R_f) must be taken into account. Therefore, in this study, the difference in real impedance at lower and higher frequencies is considered as the polarization resistance (R_p). The addition of ATD and ACT to the aggressive solution leads to a change of the impedance diagrams in both shape and size, with a depressed semicircle at the high frequency part of the spectrum. As seen from Figs 4 and 5, the R_p values increase with inhibitor concentration, which can be attributed to the formation of a protective layer at the metal surface and this layer acts as a barrier for the mass and the charge transfers. The inhibition efficiency was calculated using the following equation:

$$IE\% = \frac{R_{ct^*} - R_{ct}}{R_{ct^*}} \times 100 \quad \ldots (6)$$

Where R_{Ct*} and R_{Ct} are the values of the charge transfer resistance observed in the presence and absence of inhibitor molecules. In this case, the MS corrosion takes place only on the free surface of the metal and/or within the pores due to the diffusion of dissolved oxygen or chlorine. The values of both polarization resistance and corrosion inhibition efficiency (IE %) corresponding to the EIS at 300K are given in Table 3.

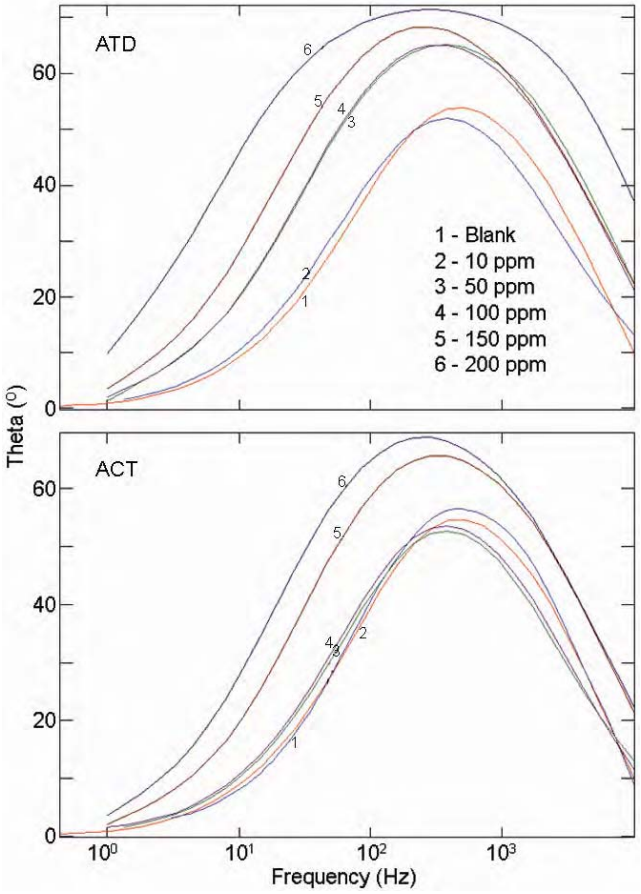

Fig.5—Bode plots of MS in 0.5M HCl in presence of different concentrations of ATD & ACT at 300K

Adsorption isotherm

The extent of corrosion inhibition depends on the surface conditions and the mode of adsorption of the inhibitors[26]. Under the assumptions that the corrosion of the covered parts of the surface is equal to zero and that the corrosion takes place only on the uncovered parts of the surface (i.e. inhibitor efficiency is due mainly to the blocking effect of the adsorbed species), the degree of surface coverage θ has been estimated from the chemical and electrochemical techniques employed in this study as follows θ = I (%)/100 (assuming a direct relationship between surface coverage and inhibition efficiency). The adsorption on the corroding surfaces never reaches the real equilibrium and tends to reach an adsorption steady state. However, when the corrosion rate is sufficiently small, the adsorption steady state has a tendency to become a quasi-equilibrium state. In this case, it is reasonable to consider the quasi-equilibrium adsorption in thermodynamic way using the appropriate equilibrium adsorption isotherms. Basic information on the interaction between the inhibitor and the mild steel surface can be provided by the adsorption isotherm. In order to obtain the isotherm, the linear relation between the values of θ and the inhibitor concentration (C_{inhi}) must be found. Attempts were made to fit the θ values to various isotherms including Langmuir, Temkin, Flory–Huggins, Dahar– Flory–Huggins and Bockris–Swinkel. By far the best fit is obtained with Temkin isotherm (log C versus log θ) and Langmuir isotherm (C versus C/θ) and is shown in Fig. 6.

Quantum chemical calculations

The optimized structures for the compounds ATD and ACT in their ground state and highest occupied molecular orbital (HOMO) and lowest unoccupied molecular orbital (LUMO) are given in Fig. 7.

Table 3—AC impedance data of mild steel (ATD & ACT) at 300K in 0.5 M H Cl solution

Inhibitor	Conc. ppm	R_{ct} Ω cm^{-2}	C_{dl} μF cm^{-2}	R_{Soln}	i_{corr} μA cm^{-2}	η %	C.R mils/yr	Surface coverage θ
	Blank	395	117	1.748	0.0763	-	51.9	-
	10	436.5	80.7	1.884	0.0598	47.45	27.27	0.4745
	50	1057	106	2.255	0.0247	78.30	11.26	0.7830
ATD	100	1096	81.43	2.427	0.0238	79.08	10.86	0.7907
	150	2543	68	2.086	0.0103	90.98	4.68	0.9098
	200	1985	69	2.490	0.0131	90.37	4.99	0.9037
	10	1312	110.9	1.641	0.0199	68.19	16.509	0.6819
	50	1307	44.90	1.973	0.0199	82.57	9.045	0.8257
ACT	100	2117	61.48	1.611	0.0123	82.45	9.1074	0.8245
	150	2014	46.97	1.782	0.012	89.16	5.6267	0.8915
	200	1974	45.30	1.695	0.013	90.12	5.103	0.9016

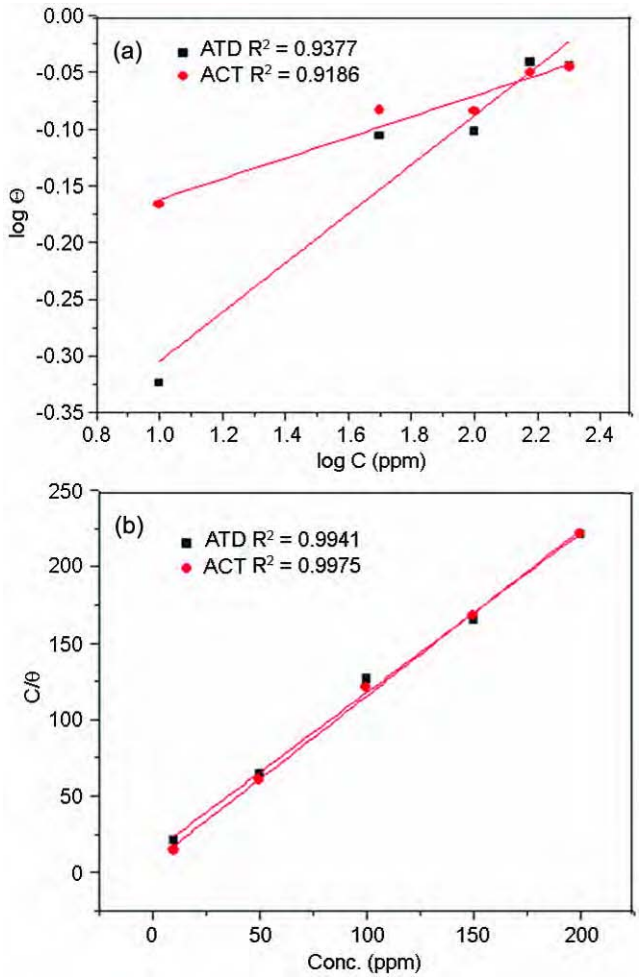

Fig.6—Temkin isotherm (a) and Langmuir isotherm (b) of ATD and ACT on surface of mild steel in 0.5M HCl at 300 K

Global reactivity

The frontier orbital (HOMO and LUMO) of a chemical species are very important in defining its reactivity. Fukui[25] first recognized this. A good correlation has been found between the speeds of corrosion and E_{HOMO} that is often associated with the electron-donating ability of the molecule. The literature shows that the adsorption of the inhibitor on the metal surface can occur on the basis of donor–acceptor interactions between the π-electrons of the heterocyclic compound and the vacant d-orbital of the metal surface atoms[27]. High values of E_{HOMO} have a tendency of the molecule to donate electrons to appropriate acceptor molecules with low energy, empty molecular orbital. Increasing values of E_{HOMO} facilitate adsorption and therefore enhance the inhibition efficiency, by influencing the transport process through the adsorbed layer. Similar relations are found between the rates of corrosion and $\Delta E = E_{LUMO} - E_{HOMO}$[38-40]. The energy of the lowest unoccupied molecular orbital indicates the ability of the molecule to accept electrons. The lower the value of E_{LUMO}, the more probable the molecule would accept electrons. Consequently, concerning the value of the energy of the gap (ΔE), larger values of the energy difference will provide low reactivity to a chemical species. Lower values of the energy difference will render good inhibition efficiency, because the energy to remove an electron from the last occupied orbital will be low[41-42]. In Table 4, certain quantum-chemical parameters related to the molecular electronic structure such as E_{HOMO}, E_{LUMO} and ΔE are presented. The higher value of E_{HOMO} and lower value of the gap energy (ΔE) show that ACT acts as a better inhibitor than ATD. The results for the calculations of the ionization potential (I) and the electron affinity (A) by application of the Koopmans' theorem are shown in Table 4. According to the Hartree–Fock theorem, a relationship exists between the energies of the HOMO, LUMO, ionization potential and the electron affinity as $-E_{HOMO} = I$ and $-E_{LUMO} = A$. Although no formal proof of this theorem exists within DFT, its validity is generally accepted. For χ and η, their operational and approximate definitions are $-\mu = (I+A)/2 = \chi$, $\eta = (I-A)/2$. Two systems, Fe and inhibitor, are brought together, electrons will flow from lower χ (inhibitor) to higher χ (Fe), until the chemical potentials become equal. As a first approximation, the fraction of electrons transferred[42] (ΔN) will be given by the following equation:

$$\Delta N = \frac{\chi_{Fe} - \chi_{inhi}}{2(\eta_{Fe} + \eta_{inhi})} \quad \ldots (7)$$

where Fe is the Lewis acid according to HSAB concept[43]. The difference in electronegativity drives the electron transfer, and the sum of the hardness parameters acts as a resistance[44]. In order to calculate the fraction of electrons transferred, a theoretical value for the electronegativity of bulk iron was used $\chi_{Fe} \approx 7$eV (ref. 37) and a global hardness of $\eta_{Fe} \approx 0$, by assuming that for a metallic bulk I=A (refs 44,45) because they are softer than the neutral metallic atoms. From Table 5, it is possible to observe that ACT has a lower value of global hardness than ATD.

Local selectivity

The local reactivity of ATD and ACT can be analyzed by means of the condensed Fukui function. The condensed Fukui functions and condensed local

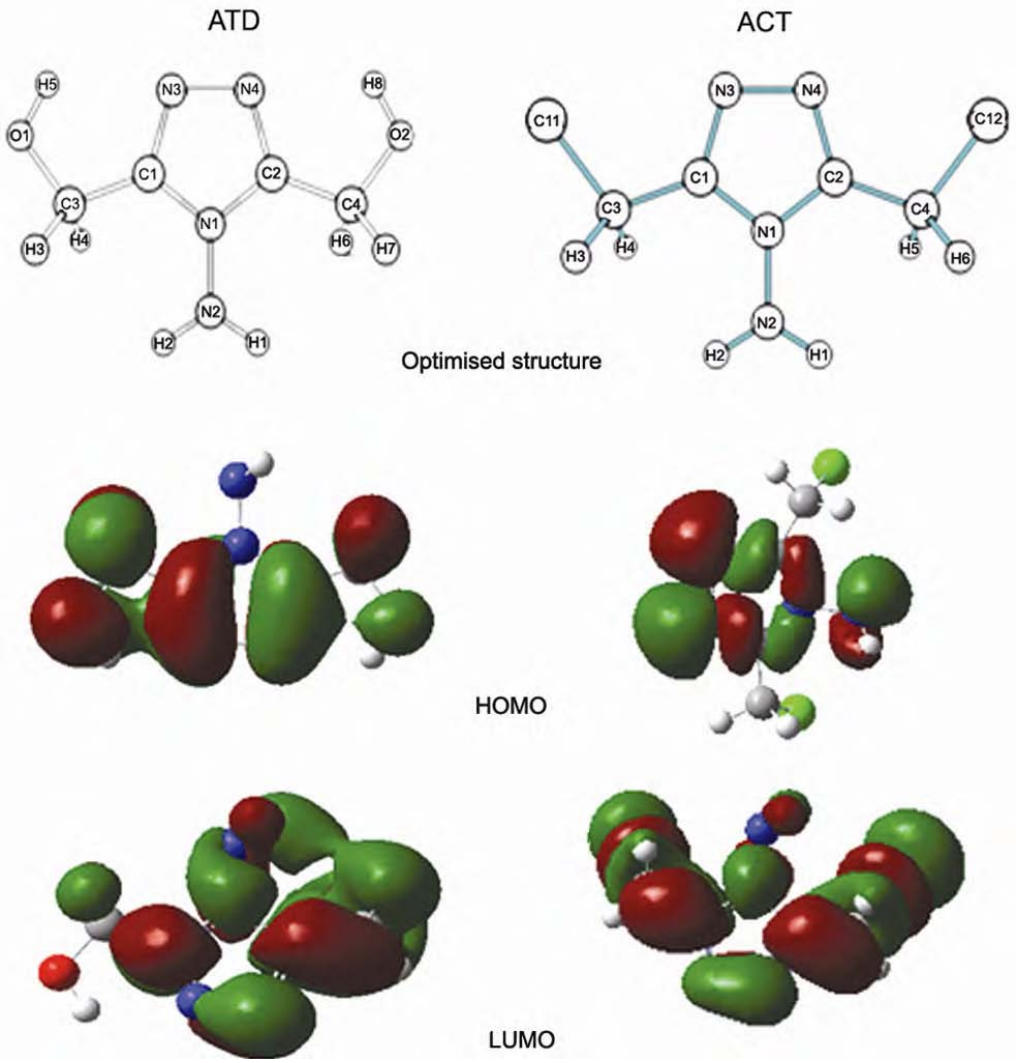

Fig. 7—Optimized structure, HOMO and LUMO of ATD and ACT

Table 4—Quantum chemical descriptors for inhibitors molecule ATD and ACT

Molecule	Total energy au	HOMO ev	LUMO ev	Δ E ev	μ	I	A	χ	η	ΔN
ATD	-526.6105	-0.1382	-6.9805	6.8423	4.9367	0.1382	6.9805	3.5504	3.4212	0.5028
ACT	-1295.3828	-1.2166	-7.2034	5.9868	5.2148	1.2166	7.2034	4.2115	2.9934	0.4660

softness indices allow us to distinguish each part of the molecule on the basis of its distinct chemical behavior due to the different substituent functional groups. Thus, the site for nucleophilic attack will be the place where the value of $\int^{+}$ is a maximum. In turn, the sight for electrophilic attack is controlled by the value of $\int^{-}$, for nucleophilic attack the most reactive site of ACT is on the C(12) and Cl (16) atoms and for molecule ADT is on the C(1) and C(2) atoms respectively. For electrophilic attack the most reactive site of ACT is on the N (7) and N (8) atoms and molecule ADT is on the N(3) and N(4) atoms respectively. These results are shown in Table 5. The condensed local softness indices Sk^{-} and Sk^{+} are related to the condensed Fukui functions. The local softness follows the same trend of Fukui functions.

Table 5—Fukui functions and local softness values for a nucleophilic and electrophilic for ACT & ATD

Atom	ACT				ATD			
	f^-	f^+	Sk^-	Sk^+	f^-	f^+	Sk^-	Sk^+
1C	0.0581	0.1269	0.0860	0.1878	0.0268	0.2664	0.0212	0.2108
2C	0.0588	0.1387	0.0870	0.2053	0.0265	0.2675	0.0209	0.2116
3N	0.0255	0.0992	0.0377	0.1468	0.2039	0.2025	0.1613	0.1602
4N	0.0902	0.0025	0.1335	0.0037	0.4807	0.0425	0.3803	0.0336
5H	0.0019	0.0079	0.0028	0.0116	0	0	0	0
6H	0.0018	0.0065	0.0026	0.0096	0	0	0	0
7N	0.3790	0.0245	0.5610	0.0363	0.1181	0.0524	0.0934	0.0414
8N	0.3750	0.0625	0.5551	0.0925	0.1186	0.0531	0.0938	0.0420
9C	-0.0005	0.0876	-0.0007	0.1296	0.0009	0.0122	0.0007	0.0096
10H	0.0013	0.0022	0.0019	0.0033	0.0032	0.0225	0.0025	0.0178
11H	0.0023	0	0.0034	0	0.0032	0.0225	0.0025	0.0178
12C	-0.0004	0.1815	-0.0006	0.2686	-	-	-	-
12O	-	-	-	-	0.0053	0.0006	0.0042	0.0004
13H	0.0032	0.0009	0.0047	0.0013	0	0	0	0
14H	0.0006	0.0022	0.0009	0.0033	0.0009	0.0123	0.0007	0.0097
15Cl	0.0017	0.0891	0.0025	0.1339	-	-	-	-
15H	-	-	-	-	0.0032	0.0225	0.0025	0.0178
16Cl	0.0016	0.1677	0.0002	0.2482	-	-	-	-
16H	-	-	-	-	0.0032	0.0226	0.0025	0.0021
17O	-	-	-	-	0.0053	0.0006	0.0042	0.0004
18H	-	-	-	-	0	0	0	0

Conclusion

(i) The inhibitor molecules show very high inhibitive efficiency for mild steel in 0.5M hydrochloric acid.

(ii) The percentage inhibitive efficiency increases with increase in concentration and decreases with longer exposure periods at 300K.

(iii) A higher coverage of the inhibitor on the metal surface is obtained in solutions with higher inhibitor concentrations.

(iv) Results of polarization studies suggest that the inhibitors (ATD and ACT) act as mixed type inhibitor.

(v) The inhibitor molecules are adsorbed on the MS surface thus blocking the reaction sites. The surface area available for the attack of the corrosive species decreases with increasing inhibitor concentrations.

(vi) The quantum chemical calculations and the electroanalytical results are in conformity with each other and the inhibitor molecule ACT acts as better inhibitor than ATD especially at lower concentrations.

Acknowledgement

One of the authors (SJ) is grateful to Council of Scientific and Industrial Research, India for providing senior research fellowship.

References

1 Sastri V S, *Corrosion Inhibitors—Principles and Applications* (Wiley, Chichester, England), 1998.
2 Growcock F B, *Corrosion*, 45 (1989) 1003
3 John S & Joseph A, *Res Chem Itermed,* DOI 10.1007/s11164-011-0468-7
4 Vreugdenhil W, Haasnoot J G, Reedijk J & Spek A L, *Inorg Chim Acta*,129 (1987) 205.
5 van Koningsbruggen P J, van Hal J W, de Graff R A G, Haasnoot J G & Reedijk J, *J Chem Soc Dalton Trans,* (1993) 2163.
6 John S, Joseph B, Balakrishnan KV, Aravindakshan K K & Joseph A, *Mater Chem Phys*, 123 (2010) 218.
7 Bentiss F, Lagrenee M, Traisnel M, Mernari B & El Attari H, *J Hetrocycl Chem*, 36 (1999) 149.
8 Mc Cafferty E, Pravadic V & Zettlemoyer A C, *Trans Faraday Soc*, 66 (1999) 237.
9 Bag S K, Chakra borty S B & Chaudhari S R, *J Indian Chem Soc,* 70 (1993) 24.
10 Ailor W H, *Hand Book of Corrosion Testing and Evaluation* (John Wiley and Sons, New York), 1971.
11 Talati J D & Modi R M, *Br Corros J,* 10 (1975) 103.
12 Talati J D & Patel G A, *Br Corros J*, 11(1976) 47.
13 Lee C, Yang W & Parr R G, *Phys Rev,* B37 (1988) 785.

14 Ignaczak A & Gomes J A N F, *Chem Phys Lett*, 257 (1996) 609.
15 Lashkari M & Arshadi M R, *Chem Phys*, 299 (2004) 131.
16 Parr R G, Donnelly R A, Levy M & Palke W E, *J Chem Phys*, 68 (1978) 3801.
17 Parr R G & Pearson R G, *J Am Chem Soc*, 105 (1983) 7512.
18 Yang W & Parr R G, *Proc Natl Acad Sci USA*, 82 (1985) 6723
19 Parr R G & Yang W, *J Am Chem Soc*, 106 (1984) 4049.
20 Yang W & Mortier W J, *J Am Chem Soc*, 108 (1986) 5708.
21 Becke A D, *J Chem Phys*, 98 (1993) 5648
22 John S & Joseph A, *Mater Chem Phys*, DOI 10.1016/ j.matchemphys.2012.02.020.
23 Lee C, Yang W & Parr R G, *Phys Rev B*, 37 (1988) 785.
24 de Proft F, Martin J M L & Geerlings P, *Chem Phys Lett*, 256 (1996) 400.
25 Champion F A, *Corrosion Testing Procedure*, 2nd edn (Chapman and Hall, London), 1964.
26 Fontana M G & Greene N D, *Corrosion Engineering*, (McGraw Hill) 1984.
27 Fuchs-Godec R, *Colloids Surf A: Physicochem Eng Aspects*, 280 (2006) 130.
28 Cheouani A, Hammouti B, Benhadda T & Daoudi M, *Appl Surf Sci*, 249 (2005) 375.
29 El Mehdi B, Mernari B, Traisnel M, Bentiss F & Lagrenee M, *Mater Chem Phys*, 77 (2002) 489.
30 Chetouani A, Hammouti B, Benhadda T & Daoudi M, *Appl Surf Sci*, 249 (2005) 375.
31 El Mehdi B, Mernari B, Traisnel M, Bentiss F & Lagrenee M, *Mater Chem Phys*, 77 (2002) 489.
32 El Achouri M, Kertit S, Gouttaya H M, Nciri B, Bensouda Y, Perez L, Infante M R & Elkacemi K, *Prog Org Coat*, 43(2001) 267.
33 Lorenz W J & Mansfeld F, *Corros Sci*, 31 (1986) 467.
34 John S, Joseph B, Aravindakshan K K & Joseph A, *Mater Chem Phys*, 122 (2010) 374.
35 Fukui K, Yonezawa T & Shingu H, *J Chem Phys*, 20 (1952) 722.
36 Hackerman N, Snavely E (Jr) & Payne J S (Jr), *J Appl Electrochem*, 113 (1966) 677.
37 Sastri V S & Perumareddi J R, *Corros Sci*, 53 (1997) 617.
38 Ogretir C, Mihçi B & Bereket G, *J Mol Struct: Theochem*, 488 (1999) 223.
39 Lukovits I, Kálmán E & Zucchi F, *Corrosion*, 57 (2001) 3.
40 Khalil N, *Electrochim Acta*, 48 (2003) 2635.
41 Lukovits I, Pálfi K, Bakó I & Kálmán E, *Corrosion*, 53 (1997) 915.
42 Pearson R G, *Inorg Chem*, 27 (1988) 734.
43 Pearson R G, *J Am Chem Soc*, 85 (1963) 3533.
44 Dewar M J S & Thiel W, *J Am Chem Soc*, 99 (1977) 4899.
45 Wang H, Wang X, Wang H, Wang L & Liu A, *J Mol Struct: Theochem*, 13 (2007) 147.